

**AN ATTRIBUTE ANALYSIS OF LOOTED SKELETAL REMAINS FROM  
THE SITE OF PANQUILMA IN THE LURIN VALLEY OF PERU**

An Undergraduate Research Scholars Thesis

by

COURTNEY VAN GEMERT

Submitted to Honors and Undergraduate Research  
Texas A&M University  
in partial fulfillment of the requirements for the designation as an

UNDERGRADUATE RESEARCH SCHOLAR

Approved by  
Research Advisor:

Dr. Suzanne Eckert

May 2014

Major: Anthropology

# TABLE OF CONTENTS

	Page
ABSTRACT.....	3
DEDICATION.....	4
ACKNOWLEDGEMENTS.....	5
NOMENCLATURE.....	6
CHAPTER I.....	7
INTRODUCTION.....	7
The Peruvian Central Coast and Ethnohistoric Interpretations of Ichma Culture.....	7
Panquilma.....	11
Regional Climate and Storm Systems.....	12
Environmental and Cultural Impacts on the Site.....	12
Cist Burial in Panquilma.....	14
Objective.....	15
CHAPTER II.....	17
METHODOLOGY.....	17
Field Methodology.....	17
Lab Methodology.....	21
CHAPTER III.....	24
RESULTS.....	24
Skeletal Inventory.....	24
MNI.....	25
Age.....	27

Sex.....	30
Stature .....	32
Pathology, Trauma and Degeneration.....	35
Artifact Analysis and Cultural Interpretations .....	40
CHAPTER IV .....	44
CONCLUSION.....	44
REFERENCES .....	47
FIGURE REFERENCES .....	51
TABLE REFERENCES.....	53

## **ABSTRACT**

An Attribute Analysis of Looted Skeletal Remains from the Site of Panquilma in the Lurin Valley of Peru. (May 2014)

Courtney Van Gemert  
Department of Anthropology  
Texas A&M University

Research Advisor: Dr. Suzanne Eckert  
Department of Anthropology

Panquilma is a 13th–15th century pre-Hispanic community of the Lurin Valley in Lima, Peru and is located in the hinterland of Pachacamac, an important religious center of the ancient Andes. Sector 03 is composed of hundreds of burial cists, most of which are arranged in clusters and have been heavily looted. Because of this, there is a lack of original burial context for the cist excavated over the Summer 2013 field season.

This paper addresses field and lab methodology as well as serves as an examination of osteological and artifact data collected over a period of one month in a superficial cleaning of Unit 14, a burial cist located in Funerary Sector 03 of the Panquilma Archaeological site. This area was chosen due to a large concentration of visible artifacts and human remains on the surface. The purpose in the superficial cleaning was to recover as much information as possible in a short time frame. Data collected for this paper specifically target questions concerning the minimum number of individuals, age range, sex of individuals, stature, and touches on the presence of possible pathological conditions, traumas, or degenerative processes that acted upon individuals buried there throughout their lifetimes, as well as status and burial ritual interpretations.

## **DEDICATION**

I dedicate this and future research in the Lurin Valley to descendants of the Ichma peoples. I hope to help restore some of the history that looters have left in ruins.

## **ACKNOWLEDGEMENTS**

I would like to thank Dr. Enrique Lopez-Hurtado for providing me with the amazing opportunity to be submersed in the Peruvian culture over the summer of 2013 and for sharing with me his extensive wealth of knowledge of the Ichma peoples. I would also like to thank Dr. Suzanne Eckert for her tremendous support throughout the production of this thesis. Their guidance has been paramount in shaping my research. Lastly, I want to thank my collaborator, Alysia Leon, for her continued assistance in and out of the field with excavation, data collection and analysis, as well as my mother, Tonya, father, Michael, and boyfriend, Gwyn for their assistance and encouragement. Without these wonderful people, this research opportunity would not be possible.

## NOMENCLATURE

AD	“Anno-Domini” (“The Year of Our Lord”)
ENSO	El Nino- Southern Oscillation
LIP	Late Intermediate Period
Midden	A dump for domestic waste which may consist of bones, excrement, botanical material, vermin, shells, sherds, lithics, and other artifacts and ecofacts associated with past human occupation.
MNI	Minimum Number of Individuals
PCC	Peruvian Central Coast
LI	Lincoln Index
S-3-U-14	Sector 3 Unit 14

# CHAPTER I

## INTRODUCTION

### **The Peruvian Central Coast and Ethnohistoric Interpretations of Ichma Culture**

The Peruvian Central Coast (PCC) stretches from the Casma valley in the north to the Mala valley in the south. It is composed of twelve valleys altogether, each of different expansion and productive capacities (See **Figure 1**) (López-Hurtado Orjeda, 2011). Around 1100AD, a time known as the LIP, following the breakup of the Wari Empire and before the conquest of the Inca in 1440AD, an age of kingdoms and regional confederations consisting of different sociopolitical and economic configurations existed in the PCC region. These balkanized polities ranged from chiefdom societies like the Huanca in the central highlands in which warfare and conflict was one of the most important social dynamics and expansive political society states like that of the Chimú people on the northern coast, to the focus of this research, a society of loosely integrated groups called the Ichma (López-Hurtado Orjeda, 2011).



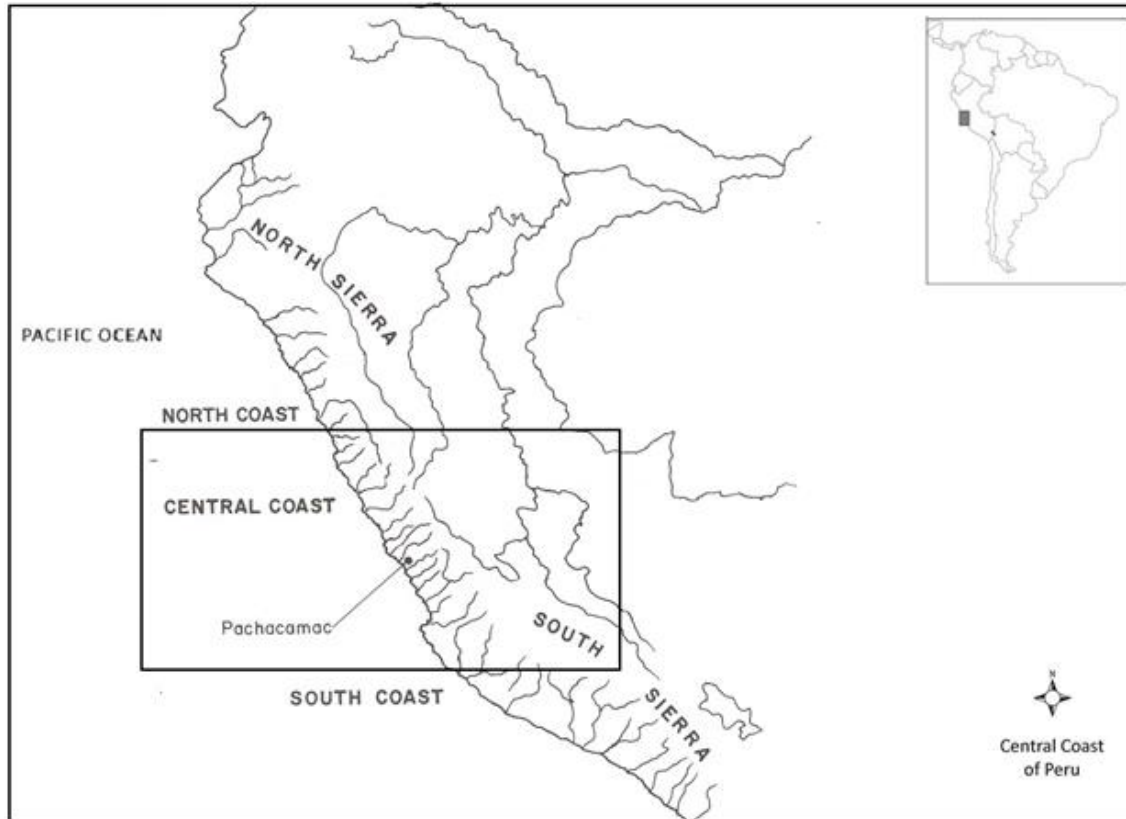


**Figure 1:** *Peruvian Central Coast (López-Hurtado Orjeda, 2011).*

The Ichma developed in the Lurin River Valley to the south of Lima and extended as far north as the Rimac River Valley. They first inhabited Pachacamac, a religious locus of the Lurin River Valley, named for a most important and feared Andean deity, Pacha Kamaq. Pilgrims would travel vast distances to worship the deity and consult the oracle in Pachacamac. It was this common belief in Pachacamac, however politically independent these pilgrims might have been, that persuaded many of them to stay and unified them into the Ichma society (López-Hurtado Orjeda, 2011).

Many archaeological interpretations have been made based on ethnohistoric accounts of the Ichma, portraying the society as a religious social hierarchy based on an ideological ascendance

of Pachacamac (Patterson, 1983, 1991). The most popular of these interpretations, proposed in the 1980's by Álvaro Bueno and Borja Jiménez-Alfaro (López-Hurtado Orjeda, 2011, Bueno, 1982, Jiménez Borja, 1992) was based on some of the most notable examples of Ichma architecture: the pyramids with ramps (López-Hurtado Orjeda, 2011). In this model, the pyramids represented the various polities that worshipped at Pachacamac and were occupied by elite Ichma priests.

Another interpretation by Peter Eeckhout (Eeckhout, 2003), is based on data recovered from the excavation of one of these pyramids. Evidenced by midden piles, intricately designed ceramics, luxury burial goods, and sacrificial victims found within and around these pyramids, Eeckhout proposed that these pyramids were rather than religious embassies, palaces of Ichma elite. In this model, the pyramids were used by the elite to hold large banquets as a wealth and power display to visiting elite. When an Ichma lord would die, he would be buried in his pyramid along with prized possessions, luxury items and even faithful servants. The existing pyramid would then be abandoned and a new one would be built for a new lord. In Eeckhout's model, the pyramids function primarily as political and economic loci, and only secondarily as religious bases (López-Hurtado Orjeda, 2011).

More data is required to evaluate which of the above interpretations are correct, or to determine if another interpretation is necessary. The research presented here can begin to help address this endeavor by widening our understanding of the demographics of the people buried at pyramid sites.

From their central location of Pachacamac the Ichma continued to grow and influence areas throughout the Lurin and Rimac river valleys like the Huaca Huantille in today's district of Magdalena del Mar, as well as Armatambo, a major urban settlement of the Ichma culture located on the left bank of the lower valley of the Rimac river, and the site from which this research is based, Panquilma, in the district of Cieneguilla, Lurin River Basin (See **Figure 2**).

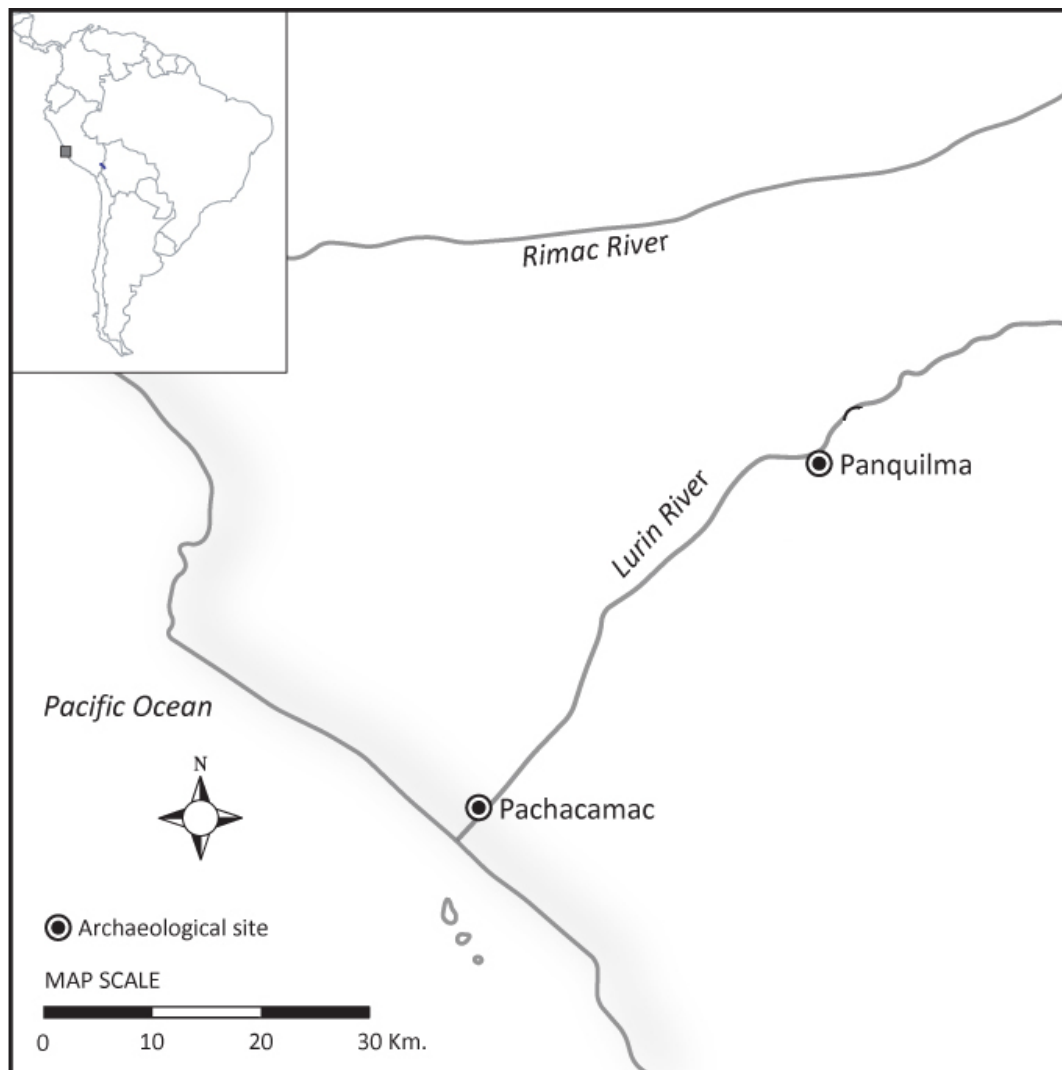


**Figure 2:** *Panquilma and Pachacamac Location (López-Hurtado Orjeda, 2011).*

## **Panquilma**

The site of Panquilma covers an area of about 300,000m<sup>2</sup> at 400 m above sea level and 28 km up valley from Pachacamac. It lies above a dry stream bed along the left bank of the Lurin River (López-Hurtado Orjeda, 2011). Panquilma is a multicomponent site occupied during the Late Intermediate and Inca Periods that is composed of a public (Sector 1) and domestic (Sector 2), as well as a non-elite domestic (Sector 3) located outside of the site's core.

Sector 1 is most notably characterized by three buildings known along the PCC as pyramids with ramps as well as a number of rectangular structures, most likely adjacent dwellings or used for storage. Sector 1 is also the area with the greatest evidence of a period of Inca occupation as evidenced by an abundance of ceramics stylized in the Inca tradition, coinciding with Ichma artifacts of the same timeframe (López-Hurtado Orjeda, 2011). This means that for awhile at least, toward the end of the LIP, these two cultures lived together in Panquilma.

Separated from the public sector and organized by causeways, Sector 2 is composed of several multi-room structures, most likely domestic elite compounds.

Sector 3 is located outside of the site's core area and lacks an prevalence of visible architectural remains as in previous sectors. Due to the sector's location in the steepest part of the valley, structures of architectural importance that might have stood here at one time would have been washed away or buried in mudslides during rainy years. This sector is thought by some to be the location of a probable non elite domestic area (López-Hurtado Orjeda, 2011, Leon, 2014), but is more commonly referred to as the Funerary Sector due to clusters of shallow rounded stone

burial cists located on the periphery of the sector. This latter interpretation was the one held by the investigators during the Summer of 2013.

### **Regional Climate and Storm Systems**

Although the PCC is located in the tropics, this region consists of an arid subtropical desert climate due to the Humboldt Current – a cold, low-salinity ocean current that flows north along the west coast of South America from the southern tip of Chile to northern Peru, and the adjacent Andes Mountain Range which prevents cumulus or cumulonimbus clouds from forming, causing a rain shadow effect (NOAA, 2005). This constant arid climate allows for optimal preservation of archaeological sites like Panquilma, yet, the region is also periodically affected by the El Niño Southern Oscillation (ENSO) – a band of anomalously warm ocean water temperatures that occasionally develops off the western coast of South America, accompanied by changes of air pressure in the east and west Pacific that cause climatic changes across the Pacific Ocean (NOAA, 2005).

### **Environmental and Cultural Impacts on the Site**

Strong El Niño events have occurred several times a century for the last 5,000 years (Sandweiss et al., 1996) although, interannual El Niño events also affect Peruvian archaeological sites like that of Pachacamac and Panquilma in detrimental ways. Torrential rain, for instance, directly erodes the surfaces of sites, especially those with positive or negative topographical relief, such as mounds or depressions. Looters' pits (and archaeological excavations that have not been backfilled or roofed) are focal points for edge erosion and pooled water that soaks into the soil and accelerates destruction of many remains (Sandweiss, 1999). These El Niño events are

evidenced in Panquilma by a large accumulation of sand due to mudslides centered in the trough of the valley that runs directly through Sector 3. Circular impressions in the sand accumulation indicate mudslide occurrence after erection of funerary cists, as well as intermittently between looter's pit establishments in the center of the valley.



**Figure 3:** Hilltop view of lunchtime during superficial cleaning in the Funerary sector valley. The area circled in blue is an example of a fresh looter's pit and the area circled in purple is an example of one of many possible funerary cists, looter's pits, or the remains of other structures possibly attributed to a non-elite domestic sector that have been covered by mudslides due to El Nin (Photo by author).

Other than the less frequent catastrophic instances of ENSO's, another large problem affecting archaeology in Panquilma is looting. Market-driven looting of archaeological material is ongoing in the Panquilma Archaeological site as well as a recognized problem in archaeological sites around the world, though agreed upon solutions remain elusive (Contreas et al., 2010). Although preservation in Panquilma and nearby Ichma occupancies is superb, frequency of looting and ENSO instances are high enough that the information able to be obtained from these sites is deteriorating faster than can be collected and explored (as evidenced in **Figure 3.**). For these

reasons, excavation of the funerary sector is imperative to the preservation of the fast eroding delicate burial remains of the Ichma culture.

### **Cist Burial in Panquilma**

Two funerary traditions coexisted in Late Ichma sites: One characterized by individual above-ground funerary structures located inside the pyramids with ramps and multi-room household compounds, and another characterized by multiple cist interments clustered outside of the populated areas (López-Hurtado Orjeda, 2011). The latter cist interment funerary tradition is the focus of the current study, as it is represented in the funerary sector of Unit 14, and one such cist was the focus of Sector 03 in the 2013 field season.

Despite ENSO activity, recurring looting of the funerary sector over the centuries and current belief that the household type of funerary tradition included the presence of costly offerings; while multiple cist interments are characterized by the modesty of their grave goods (López-Hurtado Orjeda, 2011), a superficial cleaning of Unit 14 yielded an abundance of elite burial objects such as elaborate spindle whirls, varying types of precious metal fragments and adornments (the largest and most diverse collection of artifact metal retrieved from Panquilma), a Tupu (a pin typically used to adorn clothes or hair), various colored pigments, intricately designed ceramic and shell beads, beautifully colored and detailed textiles, pottery shards, llama bone tools and metal tweezers.

## Objective

The objective of this thesis is twofold. The primary goal is an analysis and comparison to available related literature of data collected through the process of salvage archaeology to establish a minimum number of individuals, age range, sex of individuals, and to identify any pathological conditions, traumas, or degenerative processes that acted upon individuals buried there throughout their lifetimes. A second goal aims to present an interpretation of what the abundance of elite grave goods says about the people buried in this funerary cist since it is now realized that those buried in the pyramid and household funerary traditions are not the only ones buried with costly offerings (See **Figure 4** and **Figure 5**), as well as what these artifacts might say about those that survived them. Third and finally, this thesis presents recommendations for future research. The following chapters focus on these three objectives.



***Figure 4:** An intricately carved barrel-shaped wooden bead atop a wooden spindle-like object wrapped in golden thread, possibly a spindle and whorl (Photo by author).*





**Figure 5:** *A Tupu (composed of metal, most likely copper, as was common in this area during the LIP and evidenced by the green color of oxidation), discovered in cell 8 of the focus cist. (Photo by author).*

## CHAPTER II

### METHODOLOGY

#### Field Methodology

- 1 The superficial cleaning of Unit 14 of Sector 03 began with mapping of a 4x4 meter portion of a cist cluster at a mountain base.

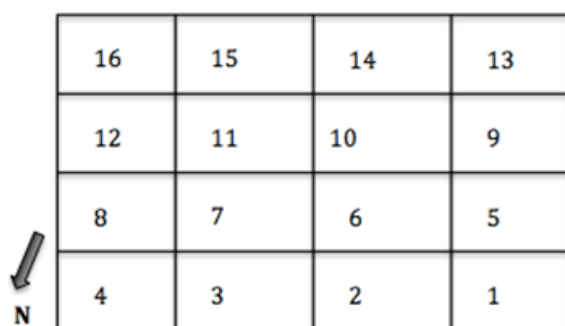


*Figure 6: Basic illustration of grid consisting of 16 1x1 meter cells (Leon, 2014).*

- 2 A grid was then established over the 4x4 meter area, although difficult due to slanting elevation and unstable loose sand and rock. The grid consisted of 16 1x1 meter cells (See **Figure 6**) constructed by myself and two colleagues utilizing two basic steel tape measures to establish length and width, a plumb bomb to keep the grid level, nylon mason's line and common round wire building nails to secure all ends of the mason's line.
- 3 After we established a grid, scaled photos were taken from the front, back, sides and above, as well as systematically (1–4, 8–5, 9–12, and 16–13) from multiple angles of each individual cell.

On the surface layer, a portion of one cist wall was visible in the center of the grid, as well as a potential second wall. The surface layer of the grid visibly consisted of large rocks, sand and assorted human bone and pottery sherds. The bones were largely concentrated at the base of the grid due to gravity (cells 1–8, with the largest concentration in cell 4).

- 4 A stratigraphic layer form and drawing were then completed for the superficial layer before cleaning.
- 5 Superficial cleaning began just outside of the grid to collect osteological remains and pottery sherds tossed out of the cists by looters. Large rocks were removed, assorted bone was moved to nearest quadrant, as well as any miscellaneous pottery sherds, textiles and botanicals. Care was taken to remove all cultural and biological material from the immediate perimeter of the grid so that no material would sustain damage from traffic and falling rock.
- 6 Cell 3 was then initiated as a test cell for cleaning due to its central base level position and high content of material. All visible bone (human and animal), pottery sherds, textiles and botanicals were collected and sorted by type of material, then tagged in the field with the following information:
  - Type of material.
  - Excavation unit.
  - Sector.
  - Context (There was no funerary context for looted material).
  - Grid context.

- Description of material if more information other than type of material was needed.
- Who the material was excavated by or the person filling out the tag (in case of cataloging discrepancies, one will know who was in charge of cataloging the particular artifact).
- Date
- Bag # in sequence (ex: bag 1 of 2)
- Number of pieces
- Weight (g).

This was done in the field to prevent context confusion once taken back to the lab for analysis. The cell was then lightly brushed for material not completely visible and those items were collected, sorted and tagged.

- 7 Sand brushed from the cell was collected in buckets and transported to sifters to separate out small items and fragments like human teeth, rodent bones, metal shards, human distal phalanges (all found frequently after sifting), botanicals, and even the occasional item of note, like spindle whirls, needles and ceramic or shell beads.
- 8 Cell 3 superficial cleaning and collection complete.
- 9 Due to high yield of material after surface collection of Cell 3 and light superficial brushing, precedence was established for a systematic cleaning of the grid.
- 10 The next step was to remove all large rocks not structurally sound since the cleaning began to prevent crushing of delicate archaeological material.

- 11 Cleaning could then continue with cells 1, 2 and 4. The same process used in cell 3 was continued in the remaining cells.
- 12 Cell 2 superficial cleaning and collection complete (This cell sits at a slightly higher elevation than adjacent cells, it also houses a large portion of the cist wall situated in the center of the grid).
- 13 Cleaning and collection completed for cell 1 then 4.
- 14 Cleaning and collection began in cell 8 and 7.
- 15 At this point a cist wall just outside the immediate vicinity of the lower left hand corner of the grid that seemed to encompass cells 3, 4, 7, 8, 11 and 12 began to take shape.
- 16 Cells 11 and 12 were then cleaned and the shape of an adjacent cist began to take shape.
- 17 An average of 5–10 bags of material was removed from the grid per day. Because of a yield higher than would be able to be processed in the lab within the remaining portion of one month, cleaning was abandoned on all cells of the grid other than cells 7, 8, 11, 12, composing one cist, as well as cells 1, 2, 3, and 4, previously completed for a superficial clean and collection.

- 18 After completion of the superficial layer, photos were again taken systematically of grid (front, back, sides and aerial view), this time with additional attention paid to the focus cist and adjacent cist, as well as others currently unexcavated in the cluster, a neighboring cluster and a few nearby isolated cists.
- 19 A new layer form and drawing were created for the completed layer.
- 20 To be thorough, although it was pretty evident that sterile soil had been reached, a test pit for excavation was attempted in cell 8.
- 21 The hypothesis was correct, sterile soil had been reached.
- 22 The archaeological recovery of looted funerary remains was complete after a superficial clean for the focus cist in Sector 03 of Unit 14.

### **Lab Methodology**

- 1 Beginning with cell 3 and moving to cells 2, 1 and then 4, bone was lightly dry brushed of all loose dirt, sand and botanical material, then separated according to type and side of the body.
- 2 After cleaning and separating, bones were wrapped in acid-free paper and placed in clean plastic storage bags according to cell.

- 3 New tags were then created for each new bag of cleaned and sided bones. The tags contain the same information as field tags, but include a site and type of material catalogue code, as well as a box number.
- 4 Limited space and material abundance only allowed for cleaning of material before packing in boxes for storage to make way for new field material.
- 5 Bones from cells 1–4 were unpacked from storage for a preliminary Minimum Number of Individuals (MNI) estimates and photos for the record (only of bones immediately necessary in determining age, sex, height, disease/injury, and MNI due to time constraints for a full analysis).
- 6 Bones from cell 8 were then lightly dry brushed, organized by type, sided, counted for the MNI and photos were taken for the record before being wrapped bagged, tagged and boxed for storage.
- 7 This same process continued for cells 7, 11, and 12.
- 8 All boxes were then pulled from storage and bones grouped by cell, were laid out on a large clean surface for a thorough second inventory.

9 Presence of injury, disease or anomaly were documented, sex, age and height were also established before bones were re-wrapped in acid-free paper and again packed away in storage.



## CHAPTER III

### RESULTS

#### **Skeletal Inventory**

The first step in the analysis of the skeletal remains retrieved from Unit 14 of Sector 3 was the compilation of an inventory that will serve both as a fundamentally important description of materials and as a basis for comparative statistical analyses (See Table 1) (Buikstra et al. 1994).

Initially, an inventory was created for each individual cell of the burial cist while analyzing remains in the lab. Later these individual inventories were combined. Due to time constraints, a comprehensive skeletal analysis was not possible so, although other miscellaneous bones are listed in the inventory, only long bones, crania and mandibles received a basic analysis. The remaining bones received a count and were examined for disease, wear and deformity. A count of each category of bone was listed in the respective column of the cell in which it was found.

These counts are the product of an initial statistical pairing of whole and fragmented bones.

Whole bone remainders were moved into a separate category and fragmented bones remainders were moved into another separate respective category. A second statistical pairing was then

conducted from a compilation of whole and fragment bone remainders from each cell (columns WRT and FRT, respectively, in Table 1). Each category of bone in Table 1 for each cell was then

laterally summed up and listed in a Sub Total (ST) category. This is where totals stop for

singular bones like mandibles, and numerous bones like ribs or vertebrae. These bones were

merely counted. Long bones and others with bilateral counterparts were statistically paired. Of

the bones in the WRT column, those without a pair were moved into the adjacent Whole

Remainder Remainder (WRR) column with a left (L) or right (R) indication. Unpaired FRT

bones were moved into their adjacent Fragment Remainder Remainder (FRR) column. Remainder bones from both categories were paired if possible and all new pairs were summed up, added to the ST totals and moved into a final Total column. All bones left unpaired were moved into a final Remainder column with an L, R, or Unidentified (U) indication. The adjacent 3 columns are an attempt at establishing an MLNI from compiled inventory data. Under the (LE) or Left Element column are the totals for left elements in each bone category, including remainders. The (RE) or Right Element column totals right elements, including remainders. Using the (L+R-P) formula, the number of confirmed pairs were subtracted from the number of unpaired bones on each side. Totals of the calculations equal the MLNI for each category of bone able to be paired. The next column in the table is an average of right and left elements:  $((L+R)/2)$ , and in the last column, the MLNI adapts an estimator called the Lincoln Index:  $((L+1)(R+1)/(P+1))-1$ . Only the integer of the solution is kept.

## **MNI**

Unfortunately, due to time constraints and the commingled, incomplete condition of the looted skeletal remains, none of the above methods could suffice for determining the minimum number of individuals within the funerary cist. Although all of the above methods seem to work out statistically, it is highly unlikely that the statistical pairs will entirely correspond to physical pairs. Instead an MNI method was applied to long bones, pelvises, mandibles and crania using this formula:  $\bar{x} ((L+R-P)+C+M)$ = the average of (( left elements + right elements – the number of confirmed pairs) + whole crania + mandibles)) to make a reasonable assumption of the minimum number of individuals necessary to account for all of the elements in the assemblage

(See **Figure 7**) (White et al., 2005). It was determined that the burial cist excavated in Unit 14 during the Summer of 2013 contained a minimum of 44 individuals.

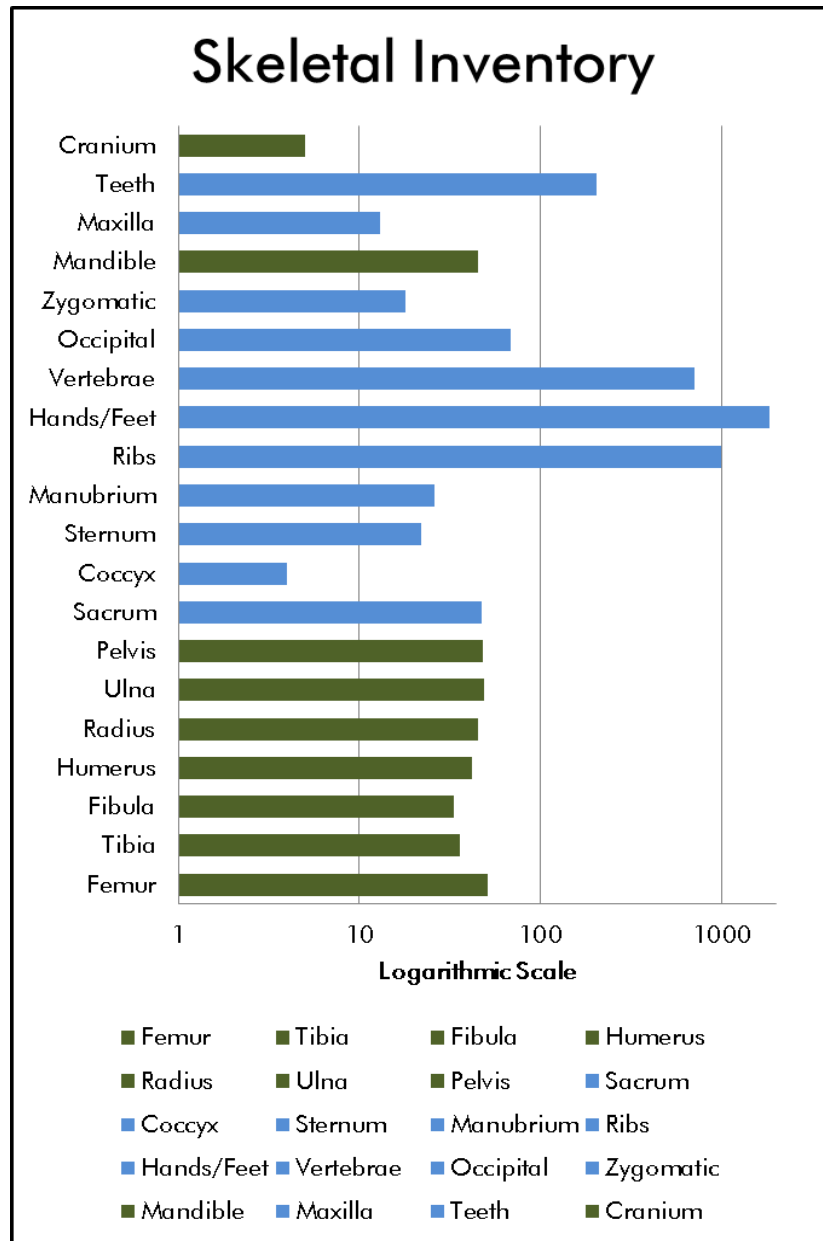


**Figure 7:** Skeletal Inventory of burial cist in U-14-S-3 and MNI using long bones, pelvises, crania and mandible (Katzenberg et al., 2008).

$$MNI \approx 44$$

## Age

Age estimations for excavated individuals at the time of death were determined through examination of cranial suture closures, degree of epiphyseal unions, as well as through morphological changes in the pubic symphysis and auricular surface of the ilium. If time had allowed, a more accurate estimate of age for a greater majority of the sample would have been possible through analysis of dental eruption, attrition rates and patterns.

Although cranial sutures generally fuse with increasing age, there is substantial closure rate variability (Buikstra et al. 1994). Degree of suture closure was recorded for 10 ectocranial sites, 4 palatal, and 3 endocranial. The age of cranial specimens intact enough for analysis were assessed using a composite of two methods, one that addresses the lateral-anterior regions, and another the cranial vault. The lateral-anterior region has proved to be a much more reliable indicator of age than the vault region (Buikstra et al. 1994).

Because of the brittle and fragmentary condition of much of the excavated remains, only 5 individuals proved to be intact enough to be evaluated through standard methods. Individual 1 (M-OAI1) received a composite score of 12 using the lateral-anterior method indicating a mean age of 46 years old. The cranial vault analysis method also yielded a score of 12, indicating a mean age of 55 years old. This individual was therefore somewhere between these two age

estimations (See **Table 1**). Individual 2 (OAI2) received a composite score of 15 using the lateral-anterior method and a score of 11 for the vault. This is the largest gap in age for an individual out of the entire sample using composite methods, between 38 and >60 years old (See **Table 2**). Individual 3 (OAI3) received a lateral-anterior composite score of 14 and a vault score of 18, indicative of an age range between 49 and 55 (See **Table 3**). A lateral-anterior score of 8 and a vault score of 6 were recorded for the 4<sup>th</sup> individual (MAI4), suggesting an age range between 38 and 43 (See **Table 4**). For the 5<sup>th</sup> individual (M-OAI5), a lateral-anterior composite score of 15 and a vault score of 12 were documented. Age ranged between 45 and 55 years old at the time of death (See **Table 5**).

**Table 1:** Cranial suture analysis (CSA) results for middle-old adult individual 1 (M-OAI1) (Buikstra et al. 1994).

CSA M-OAI1	Mean Age
Vault (comp. score: 12)	46
Lat-Ant (comp. score: 12)	55

**Table 2:** Cranial suture analysis (CSA) results for old adult female individual 2 (Buikstra et al. 1994). (OAFI2).

CSA OAI2	Mean Age
Vault (comp. score: 11)	38
Lat-Ant (comp. score: 15)	>60

**Table 3:** Cranial suture analysis (CSA) results for old adult individual 3 (OAMI3) (Buikstra et al. 1994).

CSA OAI3	Mean Age
Vault (comp score: 18)	49
Lat-Ant (comp score: 14)	55

**Table 4:** Cranial suture analysis (CSA) results for middle adult individual 4 (MAI4) (Buikstra et al. 1994).

CSA MAI4 (Fragmented)	Mean Age
Vault (comp score: 8)	38
Lat-Ant (comp score: 6)	43

**Table 5:** Cranial suture analysis (CSA) results for middle-old adult individual 5 (M-OAI5) (Buikstra et al. 1994).

CSA M-OAI5 (Fragmented)	Mean Age
Vault (comp score: 12)	45
Lat-Ant (comp score: 13)	55

**Table 6:** Age estimation based on long bone (LB) epiphyseal fusion (Buikstra et al. 1994).

Total	Infant	<15	15–22	>22	<9	14–19	14–23	<18	>24	>32	18–30	Unk
<b>Femur</b>	0	8	2	6	0	0	1	0	0	0	0	2
<b>Tibia</b>	5	9	2	7	0	0	0	0	0	0	0	7
<b>Fibula</b>	3	2	2	4	0	10	0	0	0	0	0	2
<b>Humerus</b>	3	7	0	5	9	0	4	0	0	0	0	2
<b>Radius</b>	7	7	3	9	0	8	0	0	0	0	0	1
<b>Ulna</b>	7	0	0	0	0	0	3	9	4	0	7	3
<b>Scapula</b>	5	2	5	3	0	0	0	0	0	0	0	4
<b>Clavicle</b>	4	0	0	0	0	0	0	5	0	3	11	8
<b>Sacrum</b>	0	1	0	0	0	0	0	0	2	1	1	13
<b>Pelvis</b>	11	0	3	0	0	0	2	11	2	0	0	8
<b>Total</b>	45	36	17	34	9	18	10	25	8	4	19	50
<b>MNI</b>	19	17	7	15	4	9	4	11	5	2	9	30

Fusion of postcranial epiphyses occur at known ages, however, these ages vary based on age, sex and population. The intensity of epiphyseal activity though, is concentrated between ages 15 and 23 (White et al. 2005). A total of 275 long bones from U-14-S-3 were intact enough for age analysis.

## Sex

Sex was assessed using the Standards scoring system for sexually dimorphic cranial and post cranial features (only crania, mandibles and os coxae were examined) (Buikstra et al. 1994).

Beginning with the 5 crania previously analyzed to establish age, non-metric morphology was next assessed. M-OAI1 was determined to be a male



*Figure 8: Male M-OAI1 (Photo by author)*

(See **Figure 8**). This was indicated by a thick, rounded supra-orbital margin, orbits of a more

square shape rather than rounded like females of the sample, a prominent glabellar region, a



*Figure 9: Female OAI2 (Photo by author)*

fairly sharp supra-orbital margin, a relatively smaller glabellar region as compared to males of the sample, and a minimally expressed nuchal crest. OAI3 was determined to be a male (See

nuchal crest extending a considerable distance from the occipital bone with a well-defined bony ledge, and a mastoid process extending a significant interval past the external auditory meatus. OAI2 was determined to be a female (See **Figure 9**). This assignment was indicated by a

**Figure 10).** This was indicated by a relatively thick and rounded supra-orbital margin, squarely shaped orbits, a glabella slightly larger than females of the sample, a slightly projecting nuchal crest, and an overall robusticity. Sex was more difficult to discern for MAI4 (See **Figure 11**) due to an absent post-orbital portion of the cranium, but from examination of present morphological features, this individual was estimated to be female. This



**Figure 10: Male OAI3 (Photo by author)**

was indicated by sharp supra-orbital margins, and mastoid processes projecting only a short distance below the inferior margins of the external auditory meatus. M-OAI5 was determined to



**Figure 11: Female MAI4 (Photo by author)**

be a male. This was evidenced by relatively rounded supra-orbital margins as compared to females of the sample, mastoid processes projecting a moderate distance past the auditory meatus, as well as a modestly projecting nuchal crest and a rounded, loaf-shaped glabellar prominence (See **Figure 12**).

In total, 3 males and 2 females were discerned from the intact cranial sample.



Following morphological post-cranial analysis of mandibles and os coxae, there were determined to be 18 females and 15 males, disregarding possible articulations due to time constraints. Special attention was paid to overall robusticity, relative ramus and condylar length and width, as well as amount of mental eminence projection for mandibles. Pelves were inspected for degrees of sub-pubic ventral arc, dorsal concavity, and presence of medial ridge, as well as for width of the greater sciatic notch and preauricular sulcus.



*Figure 12: Male M-OAI5 (Photo by author)*

### **Stature**

The stature estimates for individuals recovered from Unit 14 were limited to a small sample of bones because of the brittle sun-bleached and fragmentary condition of much of the remains. Of this sample, about half consisted of infant-juvenile remains. Due to incomplete epiphyseal fusion of infant-juvenile remains, multiple methods of stature analysis were utilized across the whole sample.

Initially all long bones used to establish a height estimation were divided from remains collected from all cells, then whole bones were separated from fragmentary and highly brittle bones. 165 long bones in total were analyzed (30 femura, 24 tibiae, 43 humerii, 39 radii, and 27 ulnae).

Diaphyseal lengths for bones lacking epiphyseal fusion and total lengths of the whole bones were

then measured. Height was estimated for infant-juvenile bones using the (Katsenberg and Saunders 2007) method and for adults applying the (Pomeroy and Stock 2012) method which was ideal for remains of ancient Andean ancestry. Because time and a lack of preparedness for the abundance of funerary remains and grave goods were an issue, height was determined as a range with the averaged minimum height indicating female and the averaged maximum indicating male for the adult sample (See **Figure 13**).

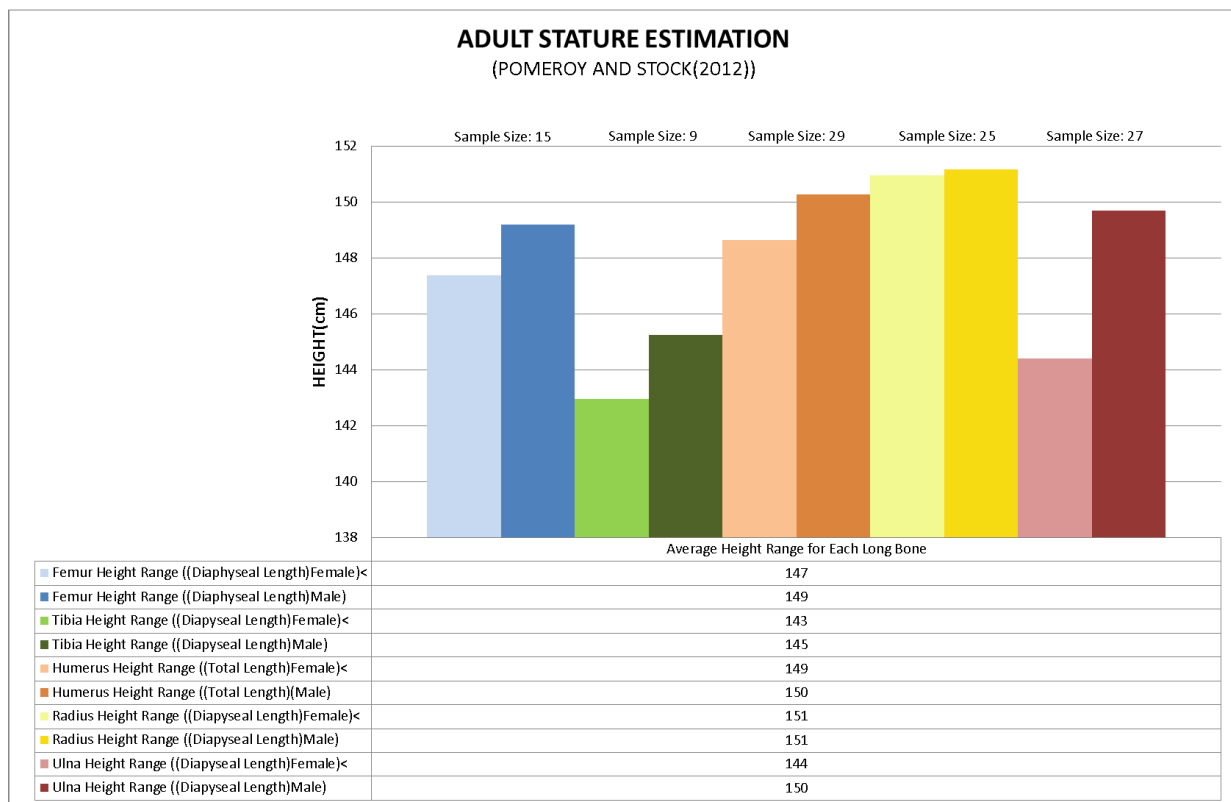


**Figure 13:** Adult stature estimation of sample based on an average range of typical ancient Andean male-female stature assigned to each bone in sample using Diaphyseal and Total Length methods (Pomeroy and Stock 2012).

For the infant and juvenile samples, an averaged minimum and maximum height were determined with a confidence interval of 80% (See **Figure 14** and **Figure 15**). The average adult femoral-based height estimations ranged from 147–149 cm, tibial-based height ranged from 143–

145 cm, humeral-based height ranged from 149–150 cm, radial-based height overlapped at 151cm, and ulnar-based height ranged from 144–150 cm. Overall, adults from this sample ranged from a height of about 143–151 cm or 4’8”–4’11”’. The average juvenile femoral-based height estimations ranged from 74–81cm, tibial-based height ranged from 84–95 cm, humeral-based height ranged from 69–91 cm, and radial-based height ranged from 77–94 cm. Ulnar measurements were not included for the juvenile stature estimation method. The overall juvenile height ranged from 69–95 cm or 2’3”–3’.

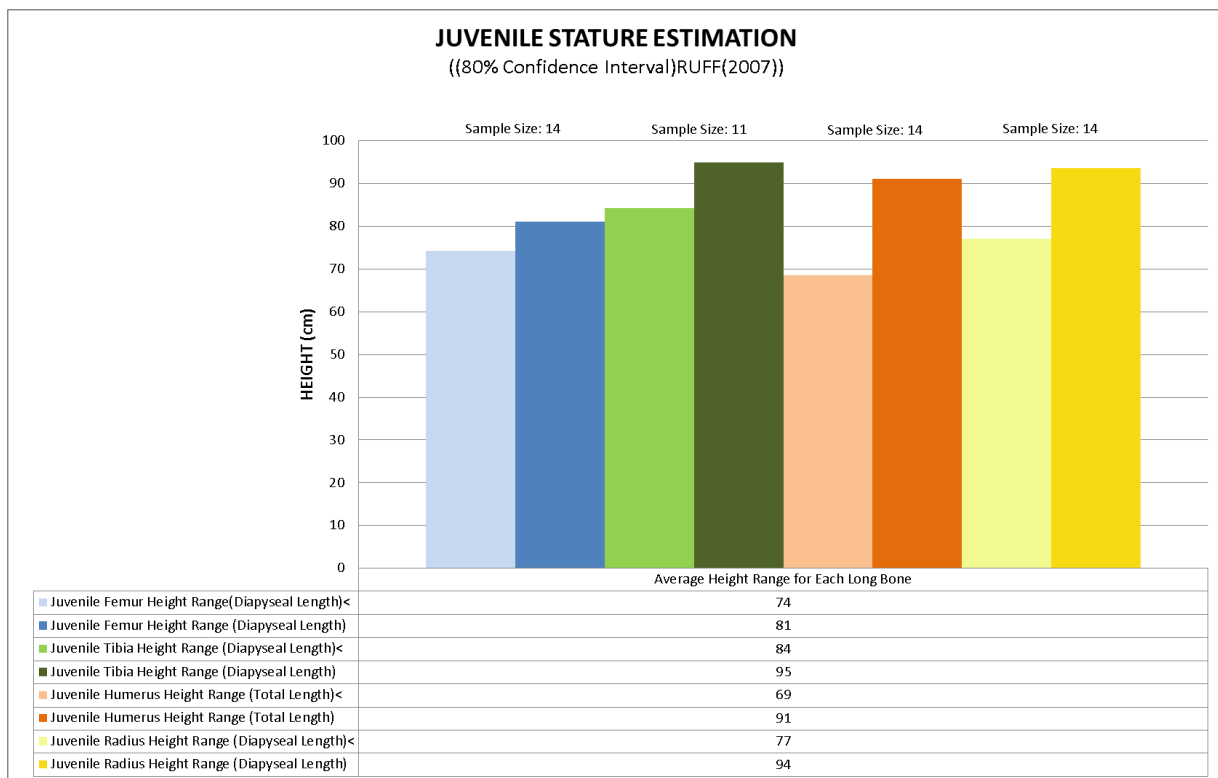


**Figure 14:** Juvenile stature estimation of sample based on an average range (80% Confidence Interval) of typical ancient Andean juvenile stature assigned to each bone in sample using Diapyseal and Total Length methods (Ruff, 2007) (Ulna does not fit these methods).

The average infant femoral-based height estimations ranged from 49–61cm, tibial-based height ranged from 47–58 cm, and humeral-based height ranged from 34–65 cm. Radial and ulnar measurements were not included for the infant stature estimation method. Average infant height ranged from 34–65 cm or 1’1”–2’2”.

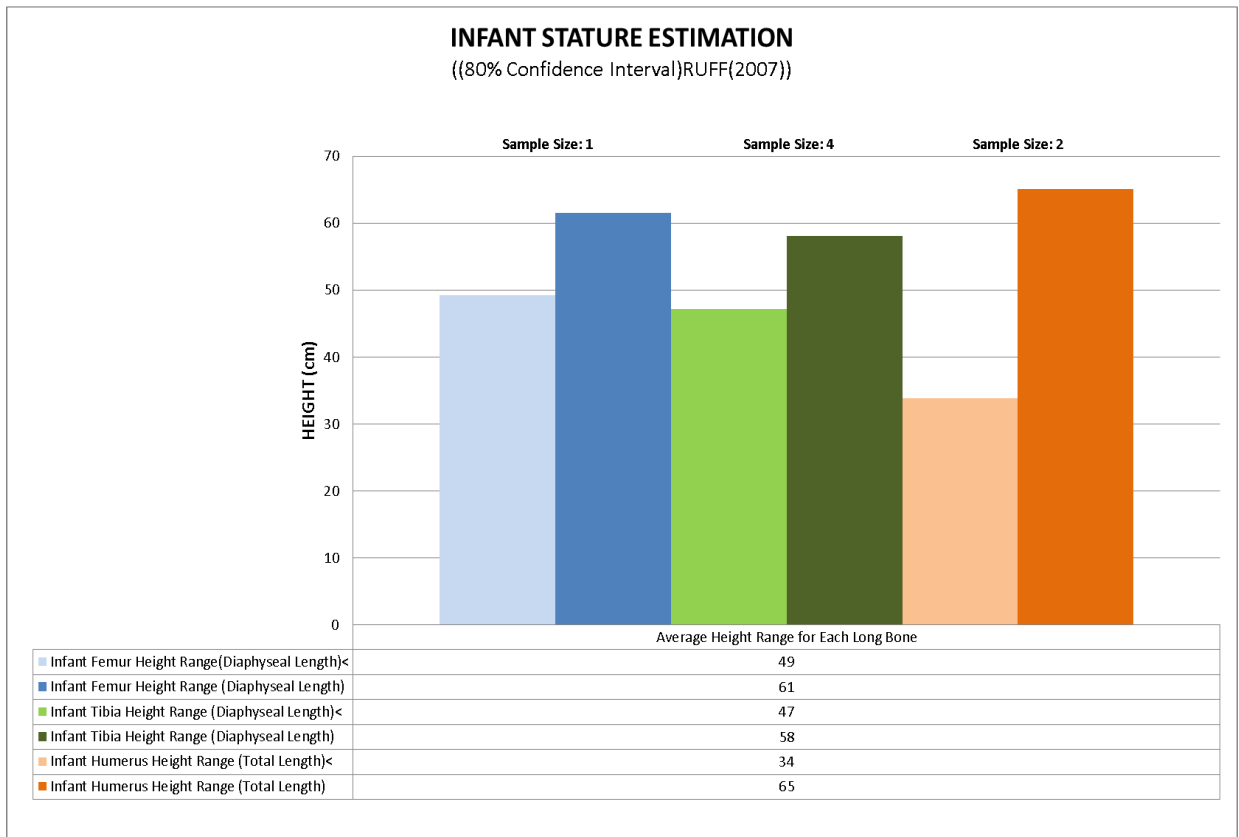


**Figure 15:** Infant stature estimation of sample based on an average range (80% confidence interval) of typical ancient Andean infant stature assigned to each bone in sample using diaphyseal and total length methods (Ruff, 2007) (radius and ulna do not fit these methods).

### Pathology, Trauma and Degeneration

Remains from Unit 14 demonstrated an array of interesting pathology, trauma and degrees of degeneration ranging from porotic hyperstosis, cribra orbitalia, rickets, osteoporotic bone loss, severe bony osteoarthritis and spinal lipping, to spinal ankylosis, alveolar resorption and tooth wear, one possible case of Eagle’s Syndrome and another possible case of cranial trepanation.

Several individuals, juveniles and infants in particular, presented varying degrees of porotic hyperstosis and cribra orbitalia, paleopathological conditions exhibiting lesions of the ectocranial surface (See Figure 16) (White et al., 2005). These conditions are expressed as macroscopic porosity on the flat bones of the cranium, namely the frontal, parietals, occipital, and hard palate (Macadam, 1987). Cribra orbitalia is similar



**Figure 16:** Evidence of porotic hyperstosis on a probable wormian bone of the occipital (Photo by author).

in appearance to porotic hyperstosis but only presents itself on the orbital roofs. It is generally accepted that the cause of these lesions is dietary in nature, most likely by an iron deficiency anemia. Groups with a higher incidence of porotic hyperstosis have traditionally been considered to be less successful in environmental adaptation or more nutritionally disadvantaged than other groups, but hypoferremia (deficiency of iron in the blood) could also be an adaptation to disease and microorganism invasion. Instead of considering porotic hyperstosis as a nutritional stress-indicator, this disease could actually be expressive of an adaptation to a pathogen load in the environment (Macadam, 1992).

U-14-S-3 also produced several juvenile and infant bones that exhibited abnormal long bone curvature and enlarged synchondroses. In conjunction with the prevalence of other nutritionally related conditions evident from this unit, the presence of this abnormal bone curvature could be suggestive of nutritional rickets. This condition is characterized by long bone deformities,

enlargement of the wrists and costochondral junctions, hypotonia, and in infants, craniotabes and delayed fontanelle closure. Rickets is a disease predominately caused by vitamin D deficiency. It first presents itself typically around 6–24 months of age, although hypocalcemia, or a lack of adequate serum calcium levels in the blood, may be evident in younger infants (Prentice, 2013).



**Figure 17:** Possible lumbar hyperlordosis and osteophytic fusion of the 5<sup>th</sup> lumbar and 1<sup>st</sup> sacral vertebrae (Photo by author).

A high frequency of osteoporotic bone loss, severe bony osteoarthritis and spinal lipping was also observed. These conditions are typically due to age-related disc degeneration but can also emerge from direct or repeated spinal trauma, or a pathological condition like spin bifida, that weakens vertebral tissue (Buikstra, 1994).

Another such related specimen was a sacrum displaying possible excessive lumbar lordosis, or a dramatically accentuated sacrolumbar

curvature, and maximum osteophytic fusion of the 5<sup>th</sup> lumbar and 1<sup>st</sup> sacral vertebrae. The fusion is indicative of the displaced position of the fifth lumbar vertebra and possibly accentuated by a constant or repeated lower back pressure or strain.

Unit 14 revealed an articulation of four highly ossified vertebrae. This is feasibly suggestive of a condition called ankylosing spondylitis (AS). This condition is a chronic inflammatory disease, slightly more common in men than women which, possibly caused by an autoimmune response, leads to inflammation in the sacroiliac joints, vertebrae and adjacent joints. Advanced cases of

AS can cause the vertebrae to fuse together and surrounding tissue to ossify, with obvious adverse impact on patient mobility and function (Sieper et al., 2009)

Brief examination of maxillae, mandibles and comingled teeth revealed a pattern of cervical-root caries accompanying root exposure found on the buccal surfaces of the posterior dentition, coinciding with the typical placement of coca quids during mastication, and significant amounts of tooth wear and alveolar resorption, indicative of a staple diet of carbohydrates like maize, potatoes and cactus (Indriati et al., 2001)

An elongated styloid process was observed in male cranium, OAI3. On average, the styloid process is between 20 and 30mm in length, but this crania displayed a structure in excess of 30mm, indicating the possibility of a rare condition known as Eagle's Syndrome. This pathology only exists in about 4% of the general population with a female-to-male predominance of 3:1 (Rinaldi, 2014). The styloid process lies in the region of the maxilla-vertebro-pharyngeal recess which also contains carotid arteries, the internal jugular vein, facial nerves, the glossopharyngeal nerve, vagal nerve, and the hypoglossal nerve. Attached to the styloid process are the muscles and ligaments which play a major role in masticating and swallowing. An elongation or ossification of the styloid process has the potential to impede on any or all of these structures depending on its



**Figure 18:** Male OAI3 with elongated styloid process, likely Eagle's Syndrome (Photo by author)

orientation resulting in symptoms such as neck and cervicofacial pain, odynophagia, dysphonia, increased salivation, dizziness, tinnitus, headache, and in extreme cases, stroke or death. Causes of Eagle's Syndrome are still unknown, but it is speculated that ectopic calcification could possibly be a cause. Abnormal calcium, phosphorus and vitamin D metabolism is very common in those with end-stage renal disease. Therefore, this calcification in nonosseous soft tissue due to abnormal calcium and phosphorus levels is commonly associated with this disorder (Gokce et al., 2008). Other possible causes are pharyngeal trauma or complications after a tonsillectomy leading to ossification of the stylohyoid muscle. Of the afore mentioned possible causes, it is in my opinion that the elongation of the styloid process belonging to OAI3 is most likely due to ectopic calcification in response to abnormal calcium, phosphorus and vitamin D metabolism because of evidence discussed previously leading to the conclusion of nutritional deficiency.

Cranium M-OAI1 exhibited a hole in the right parietal bone that measured about 6x6cm. The size, shape and consistent peripheral flaking pattern without evidence of bone resorption is likely indicative of perimortem scraping



**Figure 19:** Male M-OAI1 exhibiting 6x6cm parietal hole indicative of perimortem trepanation (Photo by author)

trepanation. Trepanation is a surgical procedure involving the intentional penetration and removal of a part of the cranial vault. The largest studied samples of trepanations are

those that derive from prehistoric Peru, with the earliest known examples dating to the Early Intermediate Period (EIP) (ca. ad 200–600) (Kurin, 2013). Motivations for performing this



procedure include physical head trauma, as well as physiological and possibly psychosomatic factors. In Andahuaylas, subadults, females, and those individuals who practiced cranial modification were withheld from this operation (Kurin, 2013).

### **Artifact Analysis and Cultural Interpretations**

Ethnohistoric sources indicate that the household items of Andean peasants were limited.

Archaeological practices have displayed the availability of only a small amount of cloth with which to wear and pottery for cooking and eating. Peasants also lacked decent baskets and sacks for grain storage, as well as tools and material necessary for weaving. Only elite members of society owned luxury items like ornate cloth, brooches, fine metal items, drinking vessels, likely for *chicha* (corn beer), made of silver or other precious metals, or the *mulla* shell (spondylus or thorny oyster, the offering and food of the gods, whose shell was used to make necklaces, breastplates, and mortuary items) (Presta, 2010). If this interpretation holds true, one would also expect to see a similar one-sided division of goods according to status in death.

Although all signs point to the belief that the household or elite type of funerary tradition included a bounty of costly offerings; while multiple cists interments include a modest amount of grave goods (López-Hurtado Orjeda, 2011), these were analyses fitting to household funerary traditions without any comparative funerary sector analysis. The 2013 superficial cleaning and analysis of U-14-S-3 has hinted at a slightly different story.

Superficial cleaning of Unit 14 began with the previous hypothesis in mind, but surprisingly, as layer after layer of dirt and botanical material were brushed and sifted from the unit, numerous beautiful treasures began to emerge among the comingled, sun-bleached remains.

Of these artifacts were copious amounts of metal discs,



**Figure 20:** Metal needle, 2 pairs of metal tweezers, and a perforated metal disc (Leon, 2014)

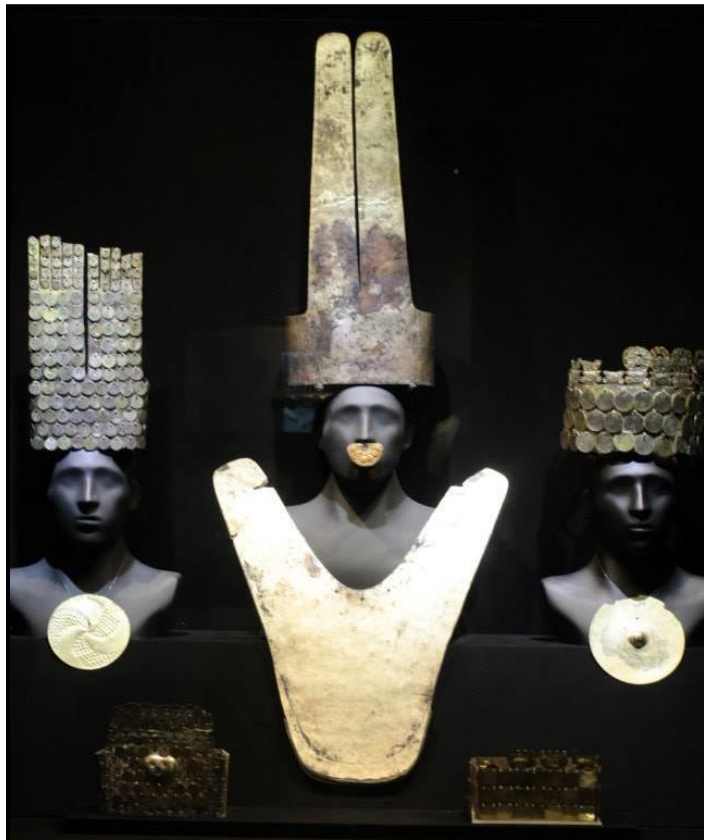


**Figure 21:** Head pieces displaying overlapping fishscale pattern of overlapping metal discs from the Museo Larco, Galeria de Oro y Joyas in Lima, Peru (Photo by author).

flakes and needles, and an intact Tupu (a long pin with a flat or ornately decorated head that was, and is still used by Andean women today to fasten wrap-around garments (See Figure 20) (Isbell 2004). Many of these metal discs had small holes punctured toward one edge and were similar to discs displayed in the *Galeria de Oro y Joyas* (Gallery of Gold and Jewels) of the Larco Museum in Lima, Peru. They are traditionally fastened to a headpiece or garment in an overlapping fish scale pattern. These discs were cast from various precious metals like gold, silver

and copper, though the discs discovered in U-14-S-3 were found to be made of a copper and gold

*tumbaga* alloy, produced by hammering copper into thin foils, occasionally with intermediate anneals.



**Figure 22:** Red, black and yellow colored belt, stylized with *Ichma* birds and fish (Leon, 2014)

These foils were then gilded by attaching gold foil. This type of Andean metalworking was relatively unknown in this time period. No reliable evidence for that matter, of Andean metallurgy has been available in Peru before the Chavin horizon (Burger et al., 1998). Other items included 3 pairs of tweezers which were used to pluck out infrequent facial hair, a custom in Pachacamac and seemingly in Panquilma as well (Squier, 1869). Metal discovered in U-14-S-3 comprises the largest collection of metal discovered at the Panquilma Archaeological site. Other items of note uncovered include substantial quantities of colored pigments, predominantly red (annatto or cinnabar) and yellow (false pepper tree). Many cranial fragments from this unit displayed smears of these pigments, possibly indicating a face painting funerary tradition. The Moche regularly used cinnabar pigment in the painting of the dead before burial (Leon, 2014). Textiles of varying qualities and designs were also discovered in U-14-S-3.

A textile of particular interest was an extraordinarily intact red, black and yellow belt illustrating a variety of stylized Ichma birds and fish. Similar bird designs were found on funerary bundles at Pachacamac. It is suggested that these motifs are of the Late Intermediate Period Chancay stylistic tradition (Leon, 2014). Other textile production related items were also found within the focus cist of U-14 such as yarn balls of various colors, wooden and metal sewing needles, a wooden spindle wrapped in gold colored thread, featuring an attached, intricately carved, anthropomorphized spindle whorl (See **Figure 4**), and four bone tools carved from llama metatarsi. These sharpened bone picks or *wichuna*, are typically used in the process of weaving. Tools of similar design were found within a grave at Machu Picchu (Eaton, 1916). Numerous shell beads, gourd containers, a nearly intact shell bead necklace constructed of various types of local shells, the whelk and chocolate most commonly found, and small fragments of spondylus beads were also discovered. This “thorny oyster” lives in warm waters between twenty and forty meters deep. Spondylus was highly valued in LIP Peruvian society for its vivid red color and difficulty to obtain. These shells were used to make adornments and were an important component of religious insignia and offerings throughout Peru’s history (Leon, 2014).



**Figure 23:** Nearly intact shell bead necklace (Leon, 2014)

## CHAPTER IV

### CONCLUSION

Although there was a lack of original burial context for the cist excavated in Unit 14 due to frequent instance of ENSOs and the destructive nature of grave looters, a wealth of knowledge was obtained from the skeletal remains and goods left behind.

A modest estimation of 44 individuals was ascertained to have been buried there, though a more accurate assessment would have been possible if time had allotted. Through long bone analysis, adult individuals were estimated to have stood between 4'8"—4'11." This approximation seems a bit short, but many adult individuals were of old age and thus, natural bone degeneration was quite evident. A majority of other adult individuals expressed inadequate nutrition, pressure and stress-induced osteoporotic bone loss, severe bony osteoarthritis and spinal degeneration which can cause a loss in height and affect the overall average.

Juveniles and infants were shown to comprise a little over half of the estimated total number of individuals. One might be quick to assume a high infant mortality rate among this civilization, but another explanation is a high fertility rate. Morphological cranial and pelvic remains were intact enough to apply standard sexing methods, indicated 18 females and 15 males, disregarding possible articulations due to time constraints. Although a small sample of the overall MNI was able to be diagnosed, the male to female distribution of Unit 14 is quite even. Combined with a relatively even age distribution, it is evident that there was no physical discrimination upon burial.

Prior to commencement of a superficial cleaning of Unit 14, the assumption was that individuals of lower status were buried in the funerary sector, while elite individuals were buried within the domestic compound or public sector. However, pathologies demonstrated among Unit 14 individuals appear to be common in remains from all sectors of Panquilma rather than unique to individuals of the funerary sector (*Leon, 2014*). Many of these similar pathologies of the nutritional and pressure-stress related variety. This is symptomatic of those who perform a great deal of physical labor and regularly consume large amounts of sugars and carbohydrates like potatoes and corn.

After a superficial cleaning in one unit of the funerary sector and sufficient analysis of human remains and funerary artifacts of a caliber not consistent with the standing hypothesis, one can easily see that a new hypothesis as to status of individuals within central coast peripheral polities during the LIP is needed. Results of artifact and human osteological remains analysis have demonstrated a virtual equality among buried individuals in Panquilma. The funerary sector, for the burial of “commoners” displayed a larger collection of precious metals and other highly sought after goods, thought to only belong to those of high status, than other more frequently excavated sectors. The elite vs. commoner hypothesis may be true in larger states of society like that of the Wari or Inca Empires, but Panquilma could quite possibly have been in an intermediate state of societal order. If this was in fact the case, then it would then be expected that there were no sharp divisions of rank, status and wealth because the Ichma lacked the defining characteristics of hierarchical civilizations (*Flanagan, 1989*).

Although the results of data exploration point to a possible hypothesis of egalitarianism, only an attribute study of a small, out-of-context sample was conducted and access to these osteological and artifact remains was fairly brief. More time and a comparative investigation of another funerary cist in Sector 3, as well as a finer, more directed analysis of remains will be needed to distinguish more definitive age, sex, stature and pathological classifications, and to further prove a possible egalitarian nature of the Ichma people.

## REFERENCES

Bueno Mendoza, A. « El antiguo valle de Pachacamac: espacio, tiempo y cultura. » Editorial Los Pinos, Lima, Perú (1982)

Buikstra, J.E., Ubelaker, D.H., Aftandilian, D. “Standards for Data Collection from Human Skeletal Remains.” Archeological Survey Research Series No. 44, Pg. 5-32 (1994)

Contreras, D., Brodie, “The Utility of Publicly-Available Satellite Imagery for Investigating Looting of Archaeological Sites in Jordan.” Journal of Field Archaeology. Vol.35, No. 1, Pg. 101 (2010)

Eaton, G.F. “The Collection of Osteological Material from Machu Picchu.” Harvard University, New Haven. (1916)

Eeckhout, P., “Ancient Monuments and Patterns of Power at Pachacamac, Central Coast of Perú.” Beitrage zur Allgemeine und Vergleichenden Archaologie. No. 23 Pgs. 139-182 (2003)

Flanagan, J.G. “Hierarchy in Simple “Egalitarian” Societies.” Annual Review Anthropology. Background. Vol. 18. Pgs. 245-266 (1989)



Gokce, C. Sisman, Y. Sipahioglu, M. “Styloid Process Elongation or Eagle’s Syndrome: Is There Any Role for Ectopic Calcification?” *European Journal of Dentistry*. No. 2. Pgs. 224-228 (July, 2008)

Indriati, E., Buikstra, J.E., “Coca chewing in prehistoric coastal Peru: dental evidence.” *American Journal of Physical Anthropology*. No.114. Pgs. 242-57. (March, 2001)

Isbell, W.H. "Mortuary Preferences: A Wari Culture Case Study from Middle Horizon Peru." *Latin American Antiquity (Society for American Archaeology)*. Vol. 15, No. 1. 3-32 (2004)

Jimenez, Borja, A. « Pachacamac: Revista de Investigaciones » Museo de la Nación (Peru). No. 1. Pgs. 125-131 (1992)

Katzenberg, A. Saunders, M. Shelley, R. “Biological Anthropology of the Human Skeleton, Second Edition” (2008).

Kurin, D. S. “Trepanation in South-Central Peru during the early late intermediate period (ca. AD 1000–1250).” *American Journal of Physical Anthropology*. No.152, Pgs. 484–494 (2013)

Leon, Alysia A. “Social Structure Inferences from Funerary Remains Located at the Site of Panquilma in Cieneguilla, Peru.” (2014)

López-Hurtado Orjeda, E.L. "Ideology and the development of social hierarchy at the site of Panquilma, Peruvian Central Coast." Pg.21-54 (2011)

Macadam, S. P. "Porotic hyperostosis: New evidence to support the anemia theory." American Journal of Physical Anthropology. No. 74, Pgs. 521-526 (1987)

"Porotic Hyperostosis: A New Perspective." American Journal of Physical Anthropology. No. 87. Pgs. 39-47 (January, 1992)

NOAA Climate Prediction Center. "Frequently Asked Questions about El Niño and La Niña". National Centers for Environmental Prediction.

[http://www.cpc.ncep.noaa.gov/products/analysis\\_monitoring/ensostuff/ensofaq.shtml#SOSCILL](http://www.cpc.ncep.noaa.gov/products/analysis_monitoring/ensostuff/ensofaq.shtml#SOSCILL). (December 19, 2005)

Patterson, T. 1983 Pachacamac: "An Andean Oracle under Inca Rule." Papers from the Second Annual Northeast Conference on Andean Archaeology and Ethnohistory. Pgs. 159-176 (1983)

"The Inca Empire: The Formation and Disintegration of a Pre-Capitalist State." Berg Publishers, Oxford. (1991)

Pomeroy, E. Stock, J. T. "Estimation of Stature and Body Mass from the Skeleton Among Coastal and Mid-Altitude Andean Populations". American Journal of Physical Anthropology. Vol. 147, Pg. 264–279(2012)

Prentice, A. "Nutritional Rickets Around the World." *The Journal of Steroid Biochemistry and Molecular Biology*. Vol. 136, Pgs. 201–206 (July, 2013)

Presta, A.M. "Undressing the Coya and Dressing the Indian Woman: Market Economy, Clothing, and Identities in the Colonial Andes, La Plata (Charcas), Late Sixteenth and Early Seventeenth Centuries." *Hispanic American Historical Review*. Vol. 90, No. 1. Pgs.41-74 (2010)

Rinaldi, V. Frequency. *Epidemiology*. Overview. Reference. Medscape.  
<http://emedicine.medscape.com/article/1447247-overview#a0199> (January, 2014)

Ruff, C. "Body size prediction from juvenile skeletal remains." *American Journal of Physical Anthropology*. Vol. 133, Pgs. 698-716 (2007)

Sandweiss, D.H.; "El Niño and the Archaeological Record in Northern Peru". *Society for American Archaeology* No. 17 Pg. 9.  
<http://www.saa.org/Portals/0/SAA/publications/SAAbulletin/17-1/index.html>(January,1999)

"Geoarchaeological Evidence from Peru for a 5000 Years B.P. Onset of El Niño."  
*Science*. No. 273: 1531-1533(1996)

Sieper, J., Braun, J. "Clinician's Manual on Ankylosing Spondylitis." Springer Healthcare Ltd.  
Introduction. Pgs. 1-3 (2009)

Squier, G.E. "A Plain Man's Tomb in Peru." Frank Leslie's Illustrated Newspaper XXVIII, No. 704. Pgs. 21-22. (March, 1869)

White, Tim D., Folkens, Pieter A., "The Human Bone Manual." Elsevier Academic Press. Pgs., 320-373 (2005)

### FIGURE REFERENCES

<b>Figure 1:</b> Peruvian Central Coast (López-Hurtado Orjeda, 2011).....	8
<b>Figure 2:</b> Panquilma and Pachacamac Location (López-Hurtado Orjeda, 2011).....	10
<b>Figure 3:</b> Hilltop view of lunchtime during superficial cleaning in the Funerary sector valley. The area circled in blue is an example of a fresh looter's pit and the area circled in purple is an example of one of many possible funerary cists, looter's pits, or the remains of other structures possibly attributed to a non-elite domestic sector that have been covered by mudslides due to El Nin (Photo by author). .....	13
<b>Figure 4:</b> An intricately carved barrel-shaped wooden bead atop a wooden spindle-like object wrapped in golden thread, possibly a spindle and whorl (Photo by author).....	15
<b>Figure 5:</b> A Tupu (composed of metal, most likely copper, as was common in this area during the LIP and evidenced by the green color of oxidation), discovered in cell 8 of the focus cist. (Photo by author). .....	16
<b>Figure 6:</b> Basic illustration of grid consisting of 16 1x1 meter cells (Leon, 2014).....	17
<b>Figure 7:</b> Skeletal Inventory of burial cist in U-14-S-3 and MNI using long bones, pelvises, crania and mandible (Katzenberg et al., 2008). .....	26
<b>Figure 8:</b> Male M-OAI1 (Photo by author) .....	30

<b>Figure 9:</b> Female OAI2 (Photo by author).....	30
<b>Figure 10:</b> Male OAI3 (Photo by author) .....	31
<b>Figure 11:</b> Female MAI4 (Photo by author) .....	31
<b>Figure 12:</b> Male M-OAI5 (Photo by author) .....	32
<b>Figure 13:</b> Adult stature estimation of sample based on an average range of typical ancient Andean male-female stature assigned to each bone in sample using Diaphyseal and Total Length methods (Pomeroy and Stock 2012).....	33
<b>Figure 14:</b> Juvenile stature estimation of sample based on an average range (80% Confidence Interval) of typical ancient Andean juvenile stature assigned to each bone in sample using Diaphyseal and Total Length methods (Ruff, 2007) (Ulna does not fit these methods). .....	34
<b>Figure 15:</b> Infant stature estimation of sample based on an average range (80% confidence interval) of typical ancient Andean infant stature assigned to each bone in sample using diaphyseal and total length methods (Ruff, 2007) (radius and ulna do not fit these methods). ...	35
<b>Figure 16:</b> Evidence of porotic hyperstosis on a probable wormian bone of the occipital (Photo by author).....	36
<b>Figure 17:</b> Possible lumbar hyperlordosis and osteophytic fusion of the 5 <sup>th</sup> lumbar and 1 <sup>st</sup> sacral vertebrae (Photo by author). .....	37
<b>Figure 18:</b> Male OAI3 with elongated styloid process, likely Eagle’s Syndrome (Photo by author).....	38
<b>Figure 19:</b> Male M-OAI1 exhibiting 6x6cm parietal hole indicative of perimortem trepanation (Photo by author) .....	39
<b>Figure 20:</b> Metal needle, 2 pairs of metal tweezers, and a perforated metal disc (Leon, 2014) ..	41

**Figure 21:** Head pieces displaying overlapping fishscale pattern of overlapping metal discs from the Museo Larco, Galeria de Oro y Joyas in Lima, Peru (Photo by author)..... 41

**Figure 22:** Red, black and yellow colored belt, stylized with Ichma birds and fish (Leon, 2014) ..... 42

**Figure 23:** Nearly intact shell bead necklace (Leon, 2014) ..... 43

### TABLE REFERENCES

**Table 1:** Cranial suture analysis (CSA) results for middle-old adult individual 1(M-OAI1 (Buikstra et al. 1994)..... 28

**Table 2:** Cranial suture analysis (CSA) results for old adult female individual 2 (Buikstra et al. 1994). (OAFI2). ..... 28

**Table 3:** Cranial suture analysis (CSA) results for old adult individual 3 (OAMI3) (Buikstra et al. 1994). ..... 28

**Table 4:** Cranial suture analysis (CSA) results for middle adult individual 4 (MAI4) (Buikstra et al. 1994). ..... 29

**Table 5:** Cranial suture analysis (CSA) results for middle-old adult individual 5 (M-OAI5) (Buikstra et al. 1994)..... 29

**Table 6:** Age estimation based on long bone (LB) epiphyseal fusion (Buikstra et al. 1994). ..... 29